Dynamic modulation of the transport properties of the $LaAlO_3/SrTiO_3$ interface using uniaxial strain

Fan Zhang,[1] Yue-Wen Fang,[2] Ngai Yui Chan,[1] Wing Chong Lo,[1] Dan Feng Li,[1] Chun-Gang Duan,[2] Feng Ding,[3] and Ji Yan Dai[1,*]

[1]*Department of Applied Physics, The Hong Kong Polytechnic University, Hung Hom, Kowloon, Hong Kong, People's Republic of China*

[2]*Key Laboratory of Polar Materials and Devices, Ministry of Education, East China Normal University, Shanghai 200062, People's Republic of China*

[3]*Institute of Textiles & Clothing, The Hong Kong Polytechnic University, Hung Hom, Kowloon, Hong Kong, People's Republic of China*

(Received 18 November 2015; revised manuscript received 1 June 2016; published 21 June 2016)

Among the interfacial transport modulations to the $LaAlO_3/SrTiO_3$ (LAO/STO) heterostructure, mechanical strain has been proven to be an effective approach by growing the LAO/STO films on different substrates with varying lattice mismatches to STO. However, this lattice-mismatch-induced strain effect is static and biaxial, hindering the study of the strain effect in a dynamic way. In this work we realize dynamic and uniaxial strain to the LAO/STO oxide heterostructure at low temperature, through mechanical coupling from a magnetostrictive template. This anisotropic strain results in symmetry breaking at the interface and induces further splitting of the electronic band structure and therefore produces different conductivities along the x and y in-plane directions. In particular, we observe that along the strained direction the interface conductivity decreases by up to 70% under a tensile strain, while it increases by 6.8% under a compressive strain at 2 K. Also, it is revealed that the modulation on the interfacial transport property can be anisotropic, i.e., the resistance changes differently when an excitation current is parallel or perpendicular to the strain direction. This approach of strain engineering provides another degree of freedom for control of transport properties of oxide heterostructures and opens an additional way to investigate strain effects in materials science.

DOI: 10.1103/PhysRevB.93.214427

I. INTRODUCTION

Since the discovery of the two-dimensional electron gas (2DEG) at the $LaAlO_3/SrTiO_3$ (LAO/STO) heterointerface, it has been very attractive for researchers to investigate modulation of transport properties of this heterostructure in different aspects [1–7]. Remarkable properties like a giant Seebeck coefficient, superconductivity, the photovoltaic effect, and unusual magnetic properties, etc., have been reported [8–15]. Among these discoveries, the effect of polar molecules on the surface of the LAO/STO heterostructure and enhanced photoresponse have been shown to be representative examples for possible device applications [16–18]. Among the interfacial transport modulations to the LAO/STO heterostructure, mechanical strain modulation of the 2DEG has attracted a great deal of attention. Both theoretical considerations and experimental studies have been carried out; however, they have revealed conflicting observations with the enhancement or suppression of the interfacial conductivity when a strain is applied [19–23]. Experimental efforts have been made by growing LAO/STO interfaces on different perovskite substrates to constrain the in-plane lattice constants of STO and LAO to various values. However, during the heteroepitaxial growth, the quality and surface state of the grown STO may have chanced to have artificial effects introduced, such as by variation of the growing temperature or oxygen pressure, and therefore there might be some uncertainties about the film crystallinity and other microstructural defects that cause deviations in the characterization results. Furthermore, the epitaxy-induced strain is essentially isotropic, manifested by simultaneous changes in both **a** and **b** crystallographic directions. This hinders unambiguous study of the effect of a uniaxial strain on the possible asymmetric transport properties due to even lower crystal symmetry. Also, the static epitaxial strain cannot provide a dynamic control on the interface and thus the 2DEG.

In this work, we report a dynamic and uniaxial modulation of strain on the LAO/STO heterostructure using a magnetostrictive material Terfenol-D [$Tb_xDy_{1-x}Fe_2$ ($x \sim 0.3$)] as a template to introduce dynamic mechanical strains onto the STO substrate. The device structure of LAO/STO/Terfenol-D is illustrated in Fig. 1(a). Terfenol-D is a material that can be elongated or compressed with a dc magnetic field, while the strain type and strength can be modulated by the magnitude and direction of the field [24] (details can be found in the Supplemental Material [25]). The LAO/STO was mounted onto Terfenol-D with epoxy after the STO was thinned to 100 μm. By applying a magnetic field, a tensile or compressive strain can be applied to the LAO/STO heterostructure. Under different types of strain, transport properties were measured with the current supplied parallel or perpendicular to the strain direction as illustrated in Figs. 1(b)–1(e). The electrodes are aluminum wires ultrasonically bonded at four corners of the sample, while the two that are on the same side as the current injection or extraction were shorted to adopt a bar configuration. The resistance is calculated as the ratio of the measured voltage and the supplied current. It should be noticed that, with this configuration of measurement, a contact resistance cannot be avoided. However, this will not affect the trend of resistance change described in our work. We have proven that the contact resistance is only a small portion of the total resistance, much less than 10% in our configuration (details can be found in the Supplemental Material [25]).

*jiyan.dai@polyu.edu.hk

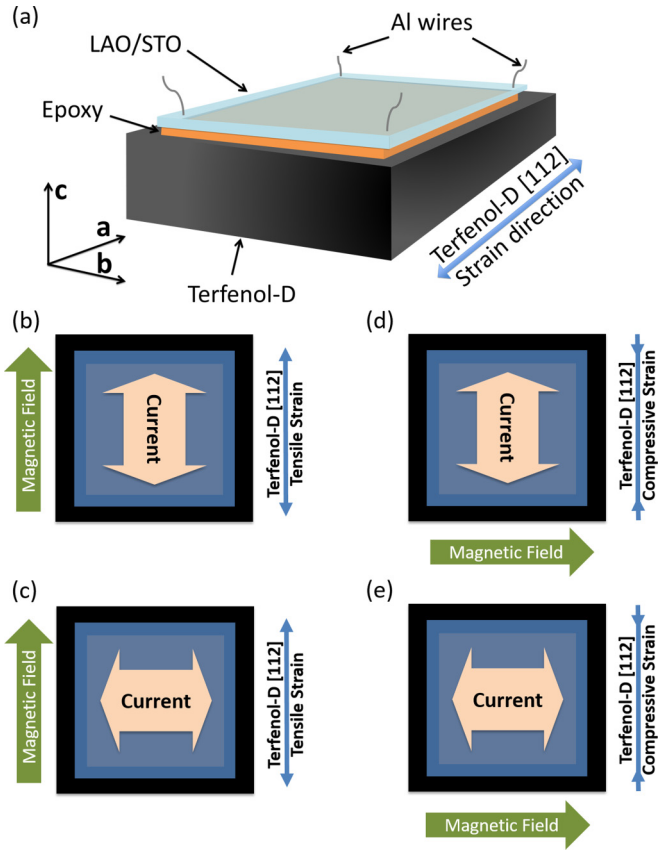

FIG. 1. Schematic illustration of anisotropic strain generation and resistance measurement. (a) The device setup of the LAO/STO attached to Terfenol-D. Measuring current is applied (b) in parallel and (c) perpendicular to the tensile strain. Measuring current is applied (d) in parallel and (e) perpendicular to the compressive strain.

At 2 K, we observe that along the strain direction the interfacial conductivity decreases by up to 70% under a tensile strain, while it increases by 6.8% under a compressive strain. These results also reveal that the modulation on the interfacial transport property can be anisotropic, i.e., the resistance changes differently when the current is parallel or perpendicular to the strain direction. This approach of strain engineering provides another degree of freedom for control of transport properties of oxide heterostructures.

II. EXPERIMENTS AND RESULTS

A. Sample preparation and characterization

$LaAlO_3$ thin films were grown on a TiO_2-terminated $SrTiO_3$ (001) substrate using reflection high-energy electron diffraction– (RHEED-) assisted laser molecular beam epitaxy (Lambda Physik COMPex 205, wavelength = 248 nm) with conditions as reported: the deposition process was conducted at 750 °C of temperature and 2×10^{-5} Pa of vacuum, followed by an *in situ* annealing at 550 °C with 1000 Pa of O_2 for 1 h before cooling down to room temperature [16]. After the STO substrate of the LAO/STO sample was milled to ~100 μm for efficient strain transfer from the template, the LAO/STO device ($2.5 \times 2.5 \times 0.1$ mm^3) was mounted on the magnetostrictive alloy Terfenol-D using M-bond epoxy which can maintain its elongation capability at 2 K. Terfenol-D's magnetic easy axis [112] is aligned in plane with the interface of LAO/STO and alongthe edges of the sample ([010] or [100] direction). Four aluminum wires were ultrasonically bonded at the corners of the square sample. To conduct the anisotropic electric characterization, the two electrodes that are on the same side of current injection or extraction were each shorted to simulate a bar configuration. The resistance is calculated as the ratio of the measured voltage and the supplied current. In a physical property measurement system (PPMS, Model 6000 by Quantum Design), an in-plane magnetic field from −5000 to +5000 Oe was applied to the Terfenol-D to introduce strain, at temperatures from 300 to 2 K. Under uniaxial strains generated both parallel and perpendicular to the current, as illustrated in Figs. 1(b)–1(e), the interfacial resistance was measured with a constant current of 500 nA. Control samples without Terfenol-D were also thinned and measured in the same manner.

Under different strains driven by various magnetic fields, we measured the temperature-dependent resistance (R-T) curve. From Fig. 2, it can be seen that, when a strain is applied to the LAO/STO heterostructure through the magnetostrictive effect, with a current parallel to the uniaxial strain direction, the conductivity of the interfacial 2DEG shows obvious change, especially when the temperature is lower than 50 K. As illustrated in Fig. 2(a), with a tensile strain driven by magnetic fields of 0, 3000, and 5000 Oe, respectively, a difference in the R-T curve emerges below 50 K. For the case of a compressive strain, the R-T curve shown in Fig. 2(b) starts splitting below 30 K. At the same time, the relative resistance change at high temperatures is negligible. We note that, especially in the low-temperature regime, the conductivity of the 2DEG is significantly tailored with a dynamic strain. At higher temperatures, the strain also shows influence on the transport properties, but much smaller in contrast to that at low temperatures. At room temperature the resistance is high, so the relative change of R is very small. The phenomenon that there is a sharp increase of resistance of LAO/STO at high temperatures could be explained as a consequence of complex coupling of the lattice, charge, and phonon [26].

At different temperatures, the resistance of the interface was also measured as the magnetic field was swept from −5000 to +5000 Oe, a range where Terfenol-D can be sufficiently elongated. Figure 3 shows the resistance as a function of the magnetic field (i.e., strain) of the sample for different temperatures from 2 to 100 K. We observe that the resistance appears to be very sensitive to the applied strain, and the resistance modulation is particularly obvious at low temperatures, which can also be seen in Fig. 2. In Fig. 3(a), one can see that the resistance increases by 70% at 2 K when the sample is under a tensile strain. By contrast, the resistance decreases by 6.8% under a compressive strain, as shown in Fig. 3(b).

Upon these observations, we systematically investigated the resistance modulations with different directions of the measuring current, which can be applied either parallel or perpendicular to the strain direction. As it can be seen from Figs. 3(a)–3(d), the behaviors of the change in resistance are different and strongly depend on the strain type and current direction. Figures 3(a) and 3(b) show the magnetic

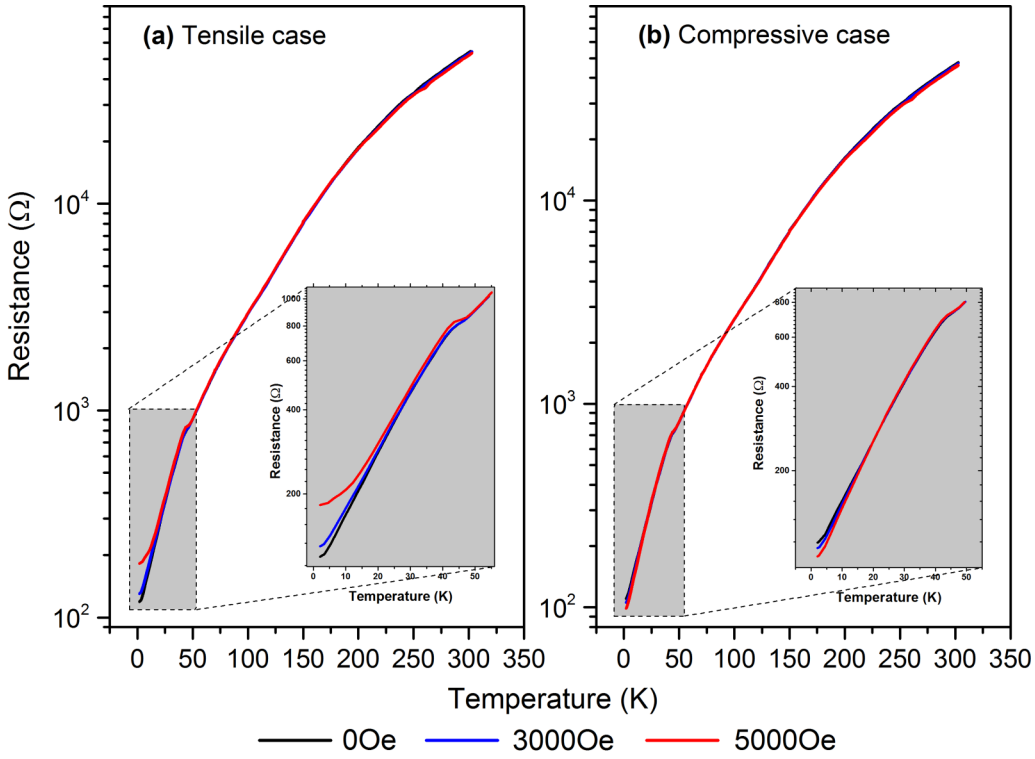

FIG. 2. Temperature-dependent resistance (R-T) curves in varied magnetic fields and strain types at temperatures ranging from 2 to 300 K. (a) LAO/STO under tensile strain. (b) Compressively strained LAO/STO.

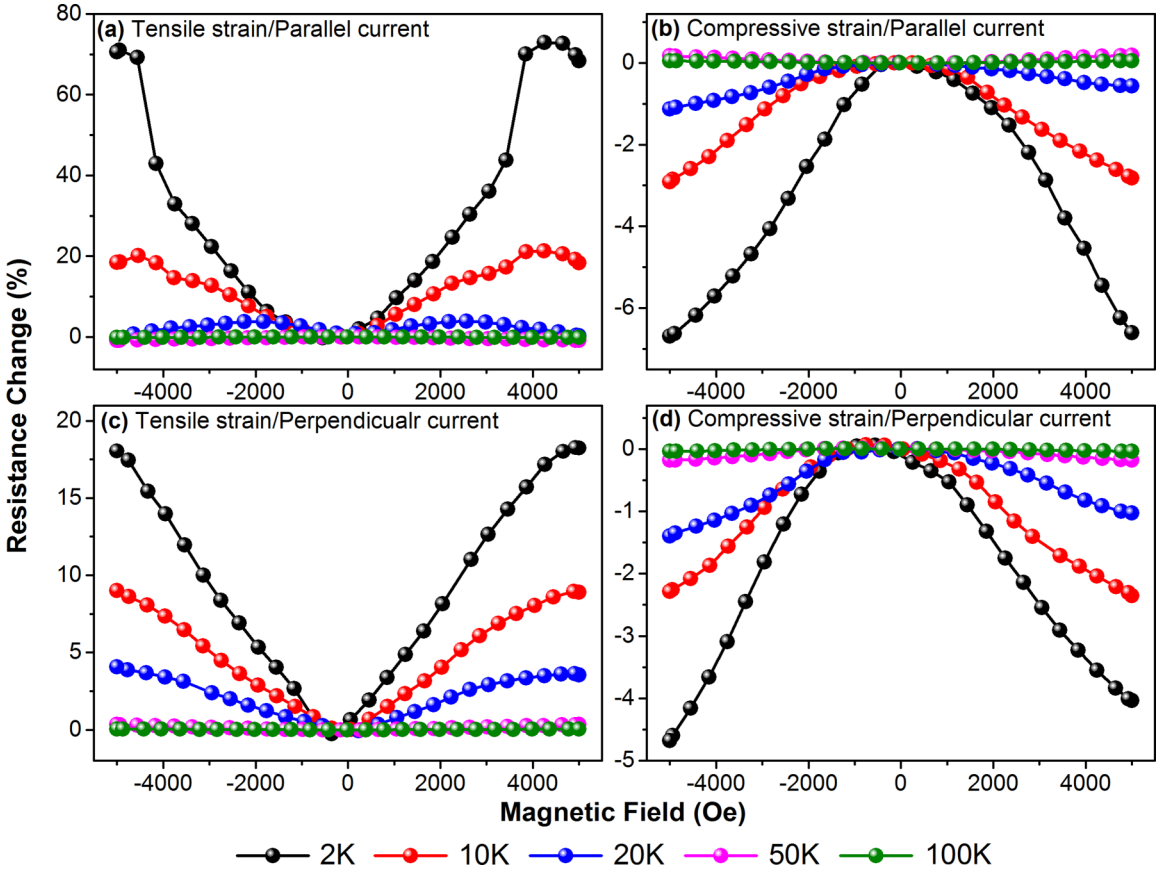

FIG. 3. Resistance change $(R–R_0)/R_0$ (%) of a LAO/STO/Terfenol-D sample. (a) Tensile strain parallel to current, as shown in Fig. 1(b); (b) compressive strain parallel to current, as shown in Fig. 1(d); (c) tensile strain perpendicular to current, as shown in Fig. 1(c); (d) compressive strain perpendicular to current, as shown in Fig. 1(e). (R_0 is the resistance in the unstrained state.)

field strength vs resistance measured with current applied in the **a** direction, which is parallel to the strain; while Figs. 3(c) and 3(d) show the magnetic field strength vs resistance measured with current applied in the **b** direction, which is perpendicular to the strain. It is worth noting that, with different current directions, there is no signature of sign inversion of the resistance change when the same type of strain is present. However, at the same temperature and strain state, the relative resistance change is smaller for the case with the current applied perpendicularly to the strain direction. At higher temperatures (200 and 300 K), the changes in resistance are very small (<0.1%) (as shown in Fig. S1 in the Supplemental Material [25]). In previous reports [27–29], very small magnetoresistance was observed at the same configuration of current and field. Therefore, at temperatures above 100 K, it is difficult to distinguish the strain effect from a pure magnetoresistance contribution. Control samples also show a magnetoresistance (MR) effect, but it is less than 0.5% when the current is parallel to the magnetic field, and less than 1.5% when the current is perpendicular to the magnetic field (as shown in Fig. S2 in the Supplemental Information [25]). The MR results are consistent with previous reports [27–29].

B. Theoretical modeling

Based on these findings, we claim that a dynamic modulation of transport properties of the 2DEG has been realized with strain from magnetostrictive coupling. The general trend of change in resistance with a tensile strain is similar to that of the reported case where LAO was grown on tensely strained STO [19,20]. However, for the compressive strain case, our result is different, as we observed a decrease of resistance. To elucidate the uniaxial strain effect on the transport properties of LAO/STO in theory, first-principles calculations within the framework of the density functional theory (DFT) method implemented in the Vienna *ab initio* Simulation Package (VASP) [30,31] were carried out. In calculations, we use the local density approximation+Hubbard U (LDA + U) method, where $U = 5$ eV for Ti d orbitals and $U = 11$ eV for La f orbitals are adopted to describe the strongly correlated electronic states. The kinetic energy cutoff is set to be 500 eV. Brillouin zone integration is sampled using a Γ-centered Monkhorst-Pack grid of $10 \times 10 \times 1$ k points in self-consistent-field calculations for $LaAlO_3/SrTiO_3$ models. For the unstrained $LaAlO_3/SrTiO_3$ slabs, the in-plane lattice constants are fixed at the optimized lattice constant of bulk $SrTiO_3$ (3.904 Å obtained by LDA + U calculation). All coordinates of atomic positions along the c direction perpendicular to the interface are fully relaxed until the forces are less than 0.01 eV/Å and concurrently the energy convergence criterion 10^{-6} eV is ensured. In particular, the effects on electronic properties brought by the in-plane compressive/tensile strains at absolute zero temperature were investigated. In order to obtain an obvious trend of strain-induced resistance changes, we applied 1% and 3% tensile and compressive strains in the calculations (even though the Terfenol-D can induce only a strain less than 1%). For comparison, an unstrained structure was also considered. We employ a symmetrical $(LaAlO_3)_4/(SrTiO_3)_{7.5}/(LaAlO_3)_4$ model with a vacuum of 20 Å width to separate the periodically repeated slabs. In the model, the strain is applied to the lattice constant a along the x direction; meanwhile the lattice constant b along the y direction is varied linearly according to Poisson's ratio [32].

The obtained density of states (DOS) is shown in Fig. 4, where zero is the reference for the Fermi level. The total 3d DOS of Ti atoms shows that the Fermi level is shifted toward the conduction bands in compressively strained LAO/STO [Fig. 4(a)] with respect to that in the unstrained LAO/STO [Fig. 4(b)]. Nevertheless, it is shifted toward the valence bands in the tensile case [Fig. 4(c)], i.e., 3% compressive strain raises the charge carrier population and 3% tensile strain reduces it. In order to demonstrate this result quantitatively, one can estimate the carrier charge concentration by integrating the DOS around the Fermi level for each case. The estimated carrier concentrations for compressive, unstrained, and tensile cases are 3.14×10^{13} cm^{-2}, 2.87×10^{13} cm^{-2}, and 2.20×10^{13} cm^{-2}, respectively, indicating that uniaxial strains can indeed effectively modulate the interfacial conductance. In addition, it can be found that Ti d_{xy} states with strong two-dimensional characteristics dominate the interfacial electronic states in all cases, as shown by the Ti d_{xy}-orbital-resolved partial density of sates (PDOS) in Fig. 4. The shift of band minima of the PDOS shows a downward band bending at the

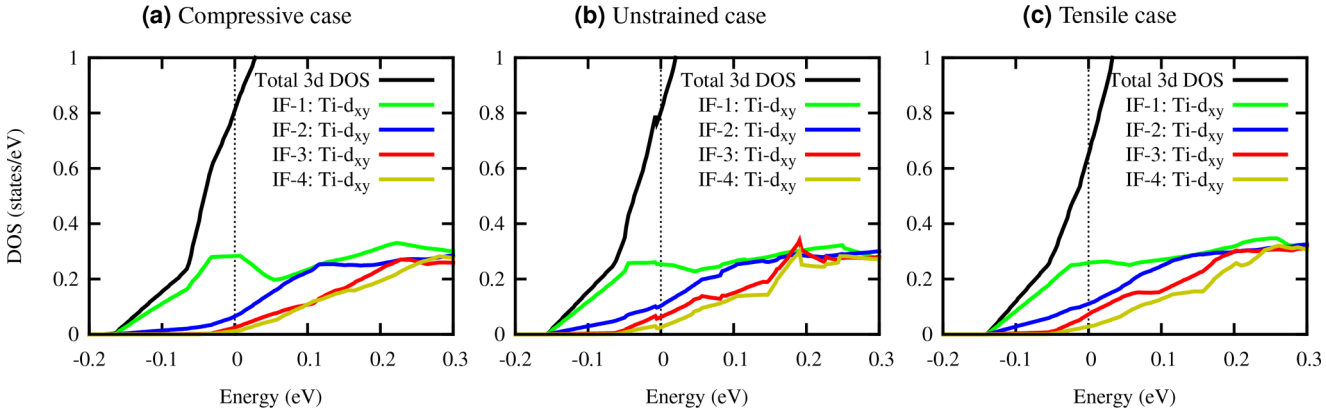

FIG. 4. Ti-d_{xy}-orbital-resolved partial density of states and total density of states (DOS) of Ti 3d in each case. (a) 3% compressive strain. (b) Unstrained. (c) 3% tensile strain. Zero on the energy axis is the reference for the Fermi level. IF-N ($N = 1,2,3,4$) is the index of the STO interfacial layer. The total 3d DOS shown here is the summation of all the Ti 3d DOSs from the four STO interfacial layers.

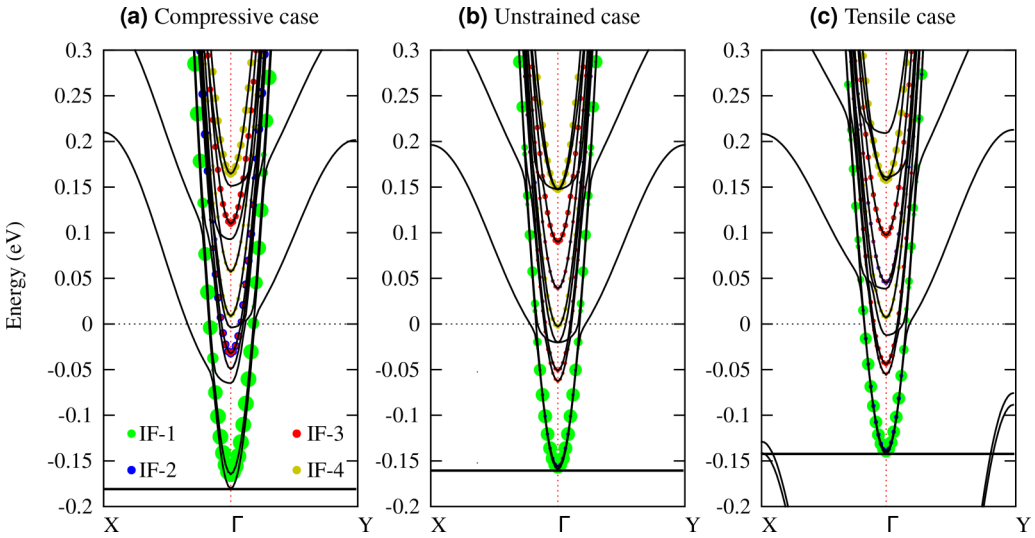

FIG. 5. Ti-d_{xy} weighted electronic band structures in each case. (a) 3% compressive strain. (b) Unstrained. (c) 3% tensile strain. Zero on the energy axis is the reference for the Fermi level. The different colors of the solid circles denote d_{xy} contributions from different STO layers.

STO side, which is suggested to be the key for formation of the 2DEG at LAO/STO interfaces [33]. In the compressive case, the quantum well created by the band bending is deepest and can confine more electrons at the interface; by contrast, fewer electrons can be trapped in the tensile state because of the narrower quantum well compared to that in unstrained LAO/STO.

Apart from the changes of interfacial conductance seen in Fig. 4, another experimentally observed phenomenon, that anisotropic interfacial conductance is introduced by uniaxial strains, can also be revealed by first-principles calculations. Figure 5 shows the band structures weighted by the Ti d_{xy} orbitals obtained in calculations. In unstrained LAO/STO, the preserved C_{4v} symmetry results in a symmetrical band structure [Fig. 5(b)]. On the other hand, asymmetrical band structures are induced [Figs. 5(a) and 5(c)] owing to the reduction of symmetry on application of uniaxial strains. This symmetry breaking drives LAO/STO into different 2DEG systems with more complex subband structures at the interfaces. Consequently, electron mobility, which is inversely proportional to the effective mass, can be significantly different in the x and y directions when uniaxial strain is applied. We thus calculate the effective masses m_x^* and m_y^*, as plotted in Fig. 6. When there is no unixial strain, m_x^* strictly equals m_y^*, indicating isotropic in-plane conductance. However, after application of uniaxial strains, notable difference of m_x^* and m_y^* can be clearly observed, reflecting the emergence of anisotropic interfacial conductance. In particular, with the increase of compressive strain along the x direction, the effective mass of electrons tends to be smaller in the x direction and larger in the y direction. However, the effective masses in the cases with tensile strains are precisely the opposite. In addition, it can also be seen from Fig. 6 that the electron mobility is much more sensitive to tensile strains than to compressive strains. These results qualitatively explain the large difference for anisotropic resistance change [maximally 70% and 18% as shown in Figs. 3(a) and 3(c)] under tensile strains and the smaller difference for anisotropic resistance change [maximally 6.8% and 4.7% as shown in Figs. 3(b) and 3(d)] under compressive strains at 2 K.

III. DISCUSSION

To present evidence that the strain is truly transferred to STO and modulates the 2DEG, we ground a bare (001) STO substrate into 30 μm of thickness and made a parallel plate capacitor with Au electrodes at both sides; this capacitor was attached on Terfenol-D as a strain sensor. As expected, a tensile strain enlarges the capacitor's area and decreases the thickness and therefore increases the capacitance, while a compressive strain induces a capacitance decrease. By the inversed capacitance changes, we proved the presence of tensile and compressive strain on the STO substrate (more details are provided in the part 4 of the Supplemental Material [25]). It should be noticed, however, that it is very difficult to

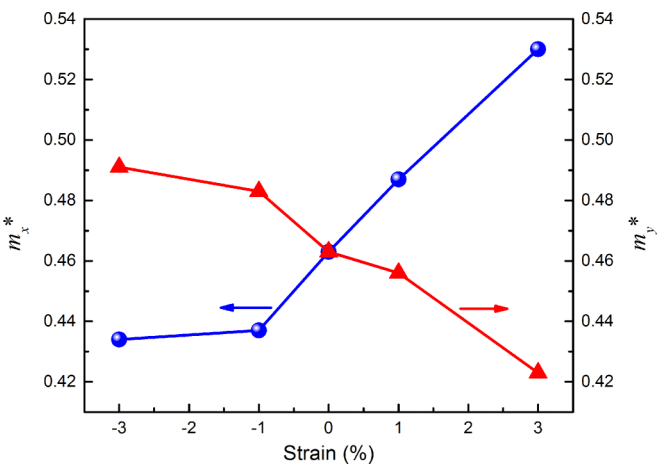

FIG. 6. Effective masses m_x^* (blue circles) and m_y^* (red triangles) in the parallel (x) and transverse (y) directions. "−" and "+" denote "compressive strain" and "tensile strain," respectively.

quantitatively measure the strain that is being transferred to the STO substrate especially at temperatures as low as 2 K, where most strain gauges do not work.

One may argue that the simulation results show only a small change of resistance under strains. This large mismatch can be further understood by considering the generation of polarization in the STO substrate under strain. Since the compressive-strain-induced resistance change is very small (the compressive strain is much smaller for Terfenol-D when a magnetic field perpendicular to the [112] direction is applied), here we consider only the tensile strain case, which induces a very large increase of resistance. As claimed in the report where LAO was grown on epitaxially strained STO [19], the tensile strain destroys the 2DEG. Jang *et al.* reported that a STO layer under tensile strain on a $DyScO_3$ substrate behaves as a relaxor with the presence of nanoscale polar regions [34]. We believe that such nanoscale polar regions could form local fields and potential barriers throughout the interface and localize the conducting interfacial electrons by scattering. This will contribute more to the increase of the interfacial resistance. Therefore, when considering the strain modulation to the interfacial conductivity at the LAO/STO interface, the STO polarization effect under strain should also be considered.

IV. CONCLUSION

To conclude, we demonstrated a dynamic and uniaxial-strain-induced modulation to the transport properties of the 2DEG at the conducting LAO/STO interface. An increase in the interfacial resistance has been observed when a uniaxial tensile strain is applied to the LAO/STO interface, while a uniaxial compressive strain produces a resistance decrease. The conductivity changes anisotropically when the measuring current is applied parallel or perpendicular to the strain direction. These results reveal the fact that appropriate anisotropic strains can result in anisotropic electron mobility and effective mass along different directions. This study provides further insights into the LAO/STO systems and paves the pathway to designingdevices made of complex oxide interfaces possessing more exotic properties. Furthermore, this method can also be applied to ultrathin films and two-dimensional materials for a study of the effects of dynamic and uniaxial strain, especially at cryogenic temperatures. We hope this method can not only motivate more discoveries on LAO/STO systems, but also stimulate new and striking findings in low-dimensional materials in other fields such as the fields of spintronics and superconductivity.

ACKNOWLEDGMENTS

This work was supported by the NSFC/RGC Grant No. N-PolyU517/14 and The Hong Kong Polytechnic University Strategic Importance Project No. 1-ZE25. The work at ECNU was supported by the National Basic Research Program of China (Grant No. 2014CB921104) and NSFC (Grant No. 61125403). All computations were conducted in the computing center at ECNU and the Chinese Tianhe-1A system at the National Supercomputer Center. The Terfenol-D alloys were provided by Dr. Choy Siu Hong.

Fan Zhang and Yue-Wen Fang contributed equally to this work.

[1] A. Ohtomo and H. Y. Hwang, Nature (London) **427**, 423 (2004).
[2] C. W. Schneider, S. Thiel, G. Hammerl, C. Richter, and J. Mannhart, Appl. Phys. Lett. **89**, 122101 (2006).
[3] S. Goswami, E. Mulazimoglu, L. M. K. Vandersypen, and A. D. Caviglia, Nano Lett. **15**, 2627 (2015).
[4] S. Thiel, G. Hammerl, A. Schmehl, C. W. Schneider, and J. Mannhart, Science **313**, 1942 (2006).
[5] B. Förg, C. Richter, and J. Mannhart, Appl. Phys. Lett. **100**, 053506 (2012).
[6] C. W. Bark, P. Sharma, Y. Wang, S. H. Baek, S. Lee, S. Ryu, C. M. Folkman, T. R. Paudel, A. Kumar, S. V. Kalinin, A. Sokolov, E. Y. Tsymbal, M. S. Rzchowski, A. Gruverman, and C. B. Eom, Nano Lett. **12**, 1765 (2012).
[7] Y. Lei, Y. Li, Y. Z. Chen, Y. W. Xie, Y. S. Chen, S. H. Wang, J. Wang, B. G. Shen, N. Pryds, H. Y. Hwang, and J. R. Sun, Nat. Commun. **5**, 5554 (2014).
[8] H. Ohta, S. Kim, Y. Mune, T. Mizoguchi, K. Nomura, S. Ohta, T. Nomura, Y. Nakanishi, Y. Ikuhara, M. Hirano, H. Hosono, and K. Koumoto, Nat. Mater. **6**, 129 (2007).
[9] N. Reyren, S. Thiel, A. D. Caviglia, L. F. Kourkoutis, G. Hammerl, C. Richter, C. W. Schneider, T. Kopp, A.-S. Rüetschi, D. Jaccard, M. Gabay, D. A. Muller, J.-M. Triscone, and J. Mannhart, Science **317**, 1196 (2007).
[10] A. D. Caviglia, S. Gariglio, N. Reyren, D. Jaccard, T. Schneider, M. Gabay, S. Thiel, G. Hammerl, J. Mannhart, and J. M. Triscone, Nature (London) **456**, 624 (2008).
[11] H. Liang, L. Cheng, X. Zhai, N. Pan, H. Guo, J. Zhao, H. Zhang, L. Li, X. Zhang, X. Wang, C. Zeng, Z. Zhang, and J. G. Hou, Sci. Rep. **3**, 1975 (2013).
[12] A. Brinkman, M. Huijben, M. van Zalk, J. Huijben, U. Zeitler, J. C. Maan, W. G. van der Wiel, G. Rijnders, D. H. A. Blank, and H. Hilgenkamp, Nat. Mater. **6**, 493 (2007).
[13] J. A. Bert, B. Kalisky, C. Bell, M. Kim, Y. Hikita, H. Y. Hwang, and K. A. Moler, Nat. Phys. **7**, 767 (2011).
[14] T. D. N. Ngo, J.-W. Chang, K. Lee, S. Han, J. S. Lee, Y. H. Kim, M.-H. Jung, Y.-J. Doh, M.-S. Choi, J. Song, and J. Kim, Nat. Commun. **6**, 8035 (2015).
[15] F. Bi, M. Huang, S. Ryu, H. Lee, C.-W. Bark, C.-B. Eom, P. Irvin, and J. Levy, Nat. Commun. **5**, 5019 (2014).
[16] K. Au, D. F. Li, N. Y. Chan, and J. Y. Dai, Adv. Mater. **24**, 2598 (2012).
[17] N. Y. Chan, M. Zhao, N. Wang, K. Au, J. Wang, L. W. H. Chan, and J. Dai, ACS Nano **7**, 8673 (2013).
[18] N. Y. Chan, M. Zhao, J. Huang, K. Au, M. H. Wong, H. M. Yao, W. Lu, Y. Chen, C. W. Ong, H. L. W. Chan, and J. Dai, Adv. Mater. **26**, 5962 (2014).
[19] C. W. Bark, D. A. Felker, Y. Wang, Y. Zhang, H. W. Jang, C. M. Folkman, J. W. Park, S. H. Baek, H. Zhou, D. D. Fong, X. Q. Pan, E. Y. Tsymbal, M. S. Rzchowski, and C. B. Eom, Proc. Natl. Acad. Sci. USA **108**, 4720 (2011).
[20] Z. Huang, Z. Q. Liu, M. Yang, S. W. Zeng, A. Annadi, W. M. Lü, X. L. Tan, P. F. Chen, L. Sun, X. Renshaw Wang, Y. L. Zhao,

C. J. Li, J. Zhou, K. Han, W. B. Wu, Y. P. Feng, J. M. D. Coey, T. Venkatesan, and Ariando, Phys. Rev. B **90**, 125156 (2014).

[21] S. Nazir and K. Yang, ACS Appl. Mater. Interfaces **6**, 22351 (2014).

[22] S. Nazir, M. Behtash, and K. Yang, Appl. Phys. Lett. **105**, 141602 (2014).

[23] Y. Du, C. Wang, J. Li, X. Zhang, F. Wang, Y. Zhu, N. Yin, and L. Mei, Comput. Mater. Sci. **99**, 57 (2015).

[24] A. E. Clark, J. P. Teter, and O. D. McMasters, J. Appl. Phys. **63**, 3910 (1988).

[25] See Supplemental Material at http://link.aps.org/supplemental/10.1103/PhysRevB.93.214427 for the magnetostriction mechanism of Terfenol-D, the unimportant influence of contact resistance, the strain-induced resistance change at relatively high temperatures, the magnetic-field-induced magnetoresistance at the LAO/STO interface, and evidence from a strained-STO-based capacitor showing that the strain is transferred to LAO/STO.

[26] C. Cancellieri, A. S. Mishchenko, U. Aschauer, A. Filippetti, C. Faber, O. S. Barisic, V. A. Rogalev, T. Schmitt, N. Nagaosa, and V. N. Strocov, Nat. Commun. **7**, 10386 (2016).

[27] Ariando, X. Wang, G. Baskaran, Z. Q. Liu, J. Huijben, J. B. Yi, A. Annadi, A. R. Barman, A. Rusydi, S. Dhar, Y. P. Feng, J. Ding, H. Hilgenkamp, and T. Venkatesan, Nat. Commun. **2**, 188 (2011).

[28] X. Wang, W. M. Lü, A. Annadi, Z. Q. Liu, K. Gopinadhan, S. Dhar, T. Venkatesan, and Ariando, Phys. Rev. B **84**, 075312 (2011).

[29] M. Diez, A. M. R. V. L. Monteiro, G. Mattoni, E. Cobanera, T. Hyart, E. Mulazimoglu, N. Bovenzi, C. W. J. Beenakker, and A. D. Caviglia, Phys. Rev. Lett. **115**, 016803 (2015).

[30] G. Kresse and J. Furthmüller, Comput. Mater. Sci. **6**, 15 (1996).

[31] G. Kresse and J. Furthmüller, Phys. Rev. B **54**, 11169 (1996).

[32] H. M. Christen, E. D. Specht, S. S. Silliman, and K. S. Harshavardhan, Phys. Rev. B **68**, 020101 (2003).

[33] Y.-L. Han, Y.-W. Fang, Z.-Z. Yang, C.-J. Li, L. He, S.-C. Shen, Z.-Z. Luo, G.-L. Qu, C.-M. Xiong, R.-F. Dou, X. Wei, L. Gu, C.-G. Duan, and J.-C. Nie, Phys. Rev. B **92**, 115304 (2015).

[34] H. W. Jang, A. Kumar, S. Denev, M. D. Biegalski, P. Maksymovych, C. W. Bark, C. T. Nelson, C. M. Folkman, S. H. Baek, N. Balke, C. M. Brooks, D. A. Tenne, D. G. Schlom, L. Q. Chen, X. Q. Pan, S. V. Kalinin, V. Gopalan, and C. B. Eom, Phys. Rev. Lett. **104**, 197601 (2010).